

Tunable Polymer Brush/Au NPs Hybrid Plasmonic Arrays Based on Host–guest Interaction

Liping Fang,[†] Yunfeng Li,[‡] Zhaolai Chen,[†] Wendong Liu,[†] Junhu Zhang,[†] Siyuan Xiang,[†] Huaizhong Shen,[†] Zibo Li,[†] and Bai Yang^{*,†}

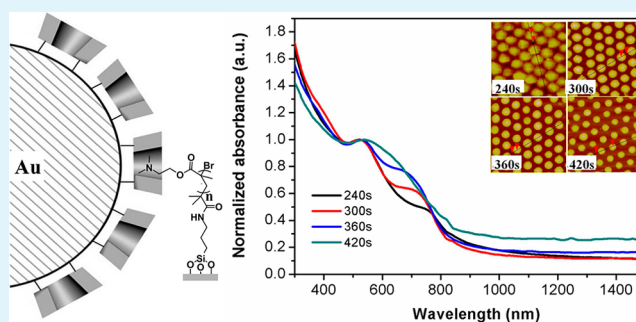
[†]State Key Laboratory of Supramolecular Structure and Materials, College of Chemistry, Jilin University, Changchun 130012, People's Republic of China

[‡]Department of Chemistry, University of Toronto, Toronto, Ontario M5S, Canada

S Supporting Information

ABSTRACT: The fabrication of versatile gold nanoparticle (Au NP) arrays with tunable optical properties by a novel host–guest interaction are presented. The gold nanoparticles were incorporated into polymer brushes by host–guest interaction between β -cyclodextrin (β -CD) ligand of gold nanoparticles and dimethylamino group of poly(2-(dimethylamino)ethyl methacrylate) (PDMAEMA). The gold nanoparticle arrays were prepared through the template of PDMAEMA brush patterns which were fabricated combining colloidal lithography and surface-initiated atom-transfer radical polymerization (SI-ATRP). The structure parameters of gold nanoparticle patterns mediated by polymer brushes such as height, diameters, periods and distances, could be easily tuned by tailoring the etching time or size of colloidal spheres in the process of colloidal lithography. The change of optical properties induced by different gold nanoparticle structures was demonstrated. The direct utilization of PDMAEMA brushes as guest avoids a series of complicated modification process and the PDMAEMA brushes can be grafted on various substrates, which broaden its applications. The prepared gold nanoparticle arrays are promising in applications of nanosensors, memory storage and surface enhanced spectroscopy.

KEYWORDS: gold nanoparticle arrays, host–guest interaction, tunable optical properties, hybrid, colloid lithography, polymer brush



INTRODUCTION

Fabrication of ordered metallic nanostructures provides the opportunities to accurately control the optical properties and have recently attracted much attention for its potential applications in a wide range of areas including nanosensors,¹ memory storage,² surface enhanced fluorescence³ and surface enhanced Raman spectroscopy.⁴ For the ordered metal arrays, the optical properties can be well controlled by varying structure parameters, such as morphology,⁵ period and spacing,^{6,7} which is fascinating characteristic of metallic nanostructures, giving us leverage to properly optimize performance of the arrays for practical applications. Because of the importance associated with nanostructured surfaces, a number of lithography techniques combined with technology of metal deposition, including electron beam lithography,⁸ photolithography,⁹ nanoimprint lithography,³ stencil lithography,⁶ and colloid lithography,¹⁰ have been developed to fabricate such metallic surfaces. However, precision instruments are often required for the metal deposition. The introduction of metal nanoparticles into patterned polymer templates provide a facile method to fabricate metallic nanostructures based on “bottom-up” strategy and low-cost electroless deposition.¹¹ Self-assembling diblock copolymer monolayer films can be

employed to produce large surface area ordered metallic nanoparticle arrays with size of dozens of nanometers resolution.¹² However, the control of structure size of the polymer template involves the variation of molecular weight of the block copolymer, which lacks convenience in structural control.¹³ Polymer brushes possess multifunctionality, multifunctional groups, and well-defined structure, which can serve as perfect template for preparation, stabilization and application of NPs,^{14,15} and many patterned polymer brushes with versatile morphologies and tunable sizes have been fabricated.¹⁶ As a result, it is convenient to fabricate metal nanoparticle arrays via patterned polymer brush templates.

In recent years, a wide range of methods have been utilized to introduce metal nanoparticles into polymer template, including hydrogen bonding interaction,¹⁷ hydrophobic interactions,¹⁸ host–guest interaction,¹⁹ electrostatic attraction,²⁰ covalent linkage,²¹ and in situ synthesis of nanoparticles in polymers.²² Among them, the use of host–guest interaction allows the arrangement of metal NPs to the polymers with

Received: August 13, 2014

Accepted: October 27, 2014

Published: October 27, 2014

good stability and controllable uniform size, and a lot of studies have been reported about the host–guest interaction between noble metal NPs and polymers.^{19,23–26} Cyclodextrin capped NPs is favored for its facile preparation, which are usually used to fabricate supramolecular aggregates by self-assembly of CD capped NPs and polymers.^{19,23,26} However, the polymers often involve complicated modification process to graft groups as guest in the host–guest interaction. Besides, few studies focus on assembling CD capped NPs on polymer thin films, although the interaction between cyclodextrins and polymer have been reported by some groups.^{27–29} Hence, it is necessary to develop a simple method to assemble nanoparticles on template of polymer films.

Here, we report a novel method to fabricate gold nanoparticle arrays by incorporating gold NPs into PDMAEMA brush patterns by host–guest interaction. The Au NPs were synthesized using β -cyclodextrin as ligand and the PDMAEMA brushes were prepared by surface-initiated atom-transfer radical polymerization. The β -cyclodextrin ligand of gold nanoparticles serves as host and dimethylamino groups of PDMAEMA serves as a guest to form hybrid films by host–guest interaction.²⁸ The direct utilization of the PDMAEMA brushes as guest avoids a series of complicated synthesis, in comparison with modification of other groups as guest in previous studies.^{26,29} Besides, the polymer brushes can be grafted on various substrates, such as silicon, silica, glass, gold, polyethylene terephthalate (PET) and so on, which extends its applications.³⁰ In our work, the structure parameters of gold nanoparticles nanopatterns mediated by polymer brushes can be arbitrarily tuned by tailoring the etching time or size of colloidal spheres in the process of colloidal lithography. The effect of various structures on the optical properties of gold nanoparticle arrays has been discussed. The PDMAEMA polymers can serve as template not only for incorporation of Au NPs but also for mineralization of a series of inorganic oxides, such as silica, titanium dioxide, and calcium phosphate.^{31–33} Inorganic oxides-metal NPs composite nanostructures can be fabricated by introducing a certain amount of Au NPs and inorganic oxides by biomineralization to the PDMAEMA patterns successively, which will indicate synergistic effect for its applications. For example, titanium dioxide-metal NPs composite nanostructures are important materials in the application of photo catalytic applications.^{34,35}

EXPERIMENTAL SECTION

Materials. Fused silica wafers were cut into $2.0 \times 2.0 \text{ cm}^2$ pieces. CuBr_2 was provided by Alfa. Aminopropyltrimethoxysilane (ATMS), 2-bromoisobutryl bromide, CuCl , 1,1,4,7,10,10-hexamethyltriethylenetetramine (HMTETA) were purchased from Aldrich. 2-(Dimethylamino)ethyl methacrylate was purchased from TCI. Dichloromethane, triethylamine, methanol, and absolute ethanol were used as received. The water used in all experiments was deionized and doubly distilled prior to use.

Preparation of PDMAEMA Brushes on Surfaces. The fused silica wafers were cleaned in the mixture of 98% H_2SO_4 /30% H_2O_2 (volumetric ratio 7:3) for 30 min under boiling (Caution: strong oxide), and then rinsed with deionized water several times, and followed by drying with an N_2 stream. Next, these wafers were placed in a sealed vessel, on the bottom of which was a few drops of ATMS. The vessel was put in an oven at 60°C for 1 h to enable the ATMS vapor to react with the $-\text{OH}$ groups on the silica wafers. After that, wafers functionalized with $-\text{NH}_2$ were immersed in the solution of 10 mL of anhydrous dichloromethane and 100 μL of triethylamine. The ATRP initiator (2-bromoisobutryl bromide, 100 μL) was added into the solution at 0°C , and the mixture was left for 1 h at this temperature then at room temperature for ~ 15 h. The wafers were

cleaned by anhydrous dichloromethane absolute ethanol for several times, and dried by N_2 flow.

For the polymerization of PDMAEMA, 8 mg (0.03 mmol) of CuBr_2 , 100 μL (0.35 mmol) of HMTETA, 2 mL of water, 2 mL of methanol, and 4 mL of DMAEMA were added into a vial, and then the mixtures were shaken in an ultrasonic bath until a homogeneous blue solution was formed. The mixtures were degassed by ultrapure nitrogen flow for 30 min. Subsequently, 25 mg (0.25 mmol) of CuCl was added into the solution, and it was shaken in an ultrasonic bath until dissolved absolutely. Lastly, the wafers with initiators were immersed in the solution from 15 min to 3 h under the nitrogen flow at room temperature. After polymerization, the samples were cleaned by absolute ethanol and deionized water for several times.

Preparation of Patterned PDMAEMA Brushes. PDMAEMA brush nanopatterns were prepared by colloidal lithography using a 2D polystyrene (PS) colloidal crystal as a mask. First, 2D PS colloidal crystals were prepared by a modified interfacial method on the wafers with PDMAEMA brush films.³⁶ The PS microspheres used in our work were 580 nm. Subsequently, oxygen reactive ion etching (RIE) operating at 10 mTorr pressure, 50 SCCM flow rate, and RF power of 30 W with an ICP power of 100 W was carried out for a length of time ranging from 240 to 420 s. Finally, PDMAEMA brush nanopatterns were obtained after the remaining PS microspheres were removed by dimethylformamide under an ultrasonic bath.

Preparation of the Composite PDMAEMA/gold NPs Arrays. The gold nanoparticles capped with beta-cyclodextrin were synthesized according to previous procedure.³⁷ briefly, 1 mL gold nanoparticles (0.5 mg/mL) and 1 mL borate buffer (pH = 9.18) were mixed in a small weighing bottle. Then the substrates grafted with PDMAEMA brushes or patterned PDMAEMA brushes were added in the mixed solution and incorporate for 8 h on table concentrator. Finally, the substrate was rinsed with deionized water several times and dried by N_2 flow.

Characterization. The atomic force microscopy (AFM) images were recorded in tapping mode with a Nanoscope IIIa scanning probe microscope from Digital Instruments under ambient conditions. The thicknesses of the PDMAEMA brush films were measured by Dektak150 surface profiler (Veeco). Transmission electron microscope (TEM) was conducted using a Hitachi H-800 electron microscope at an acceleration voltage of 200 kV with a CCD cinema. Ultraviolet visible (UV–vis) absorption spectra were obtained using a Shimadzu 3600 UV–vis–NIR spectrophotometer. X-ray Photoelectron Spectroscopy (XPS) was investigated by using ESCALAB 250 spectrometer with a mono X-ray source Al K excitation (1486.6 eV).

3. RESULTS AND DISCUSSION

Preparation and Characterization of Polymer Brush/Au NP Hybrid Films. The PDMAEMA brushes were grown on silicon substrates by ATRP reaction and the thickness of brushes can be adjusted from 22 to 130 nm through varying the polymerization duration. The gold nanoparticles were synthesized via reduction with sodium borohydride in the presence of perthiolated CD. The gold nanoparticles were introduced into PDMAEMA brushes by host–guest interaction. The calculated diameter of β -CD decorated gold nanoparticles is 4.3 nm and the UV–vis absorption spectrum of the Au NPs with absorption band at around 513 nm (Supporting Information Figure S1a). The average Au nanoparticle is covered by ~ 22 covalently attached β -CD ligands estimated by previous report.³⁸ After incorporated in the polymer brushes, the gold nanoparticles are close to each other and the absorption band is red-shifted to 538 nm (Supporting Information Figure S1b). It is mainly attributed to the perturbation of the dielectric constant around the nanoparticles, and the encompassment of the polymer brushes increases the surrounding dielectric constant of the Au NPs, resulting in red shift of the spectra.²¹

To further investigate the distribution of Au NPs in the brush films, AFM was used to analyze hybrid films. The surface of the bare PDMAEMA brushes appears homogeneous and smooth, and the surface morphology become rough after introducing Au NPs within the brush layer (Figure 1). In the meantime, the

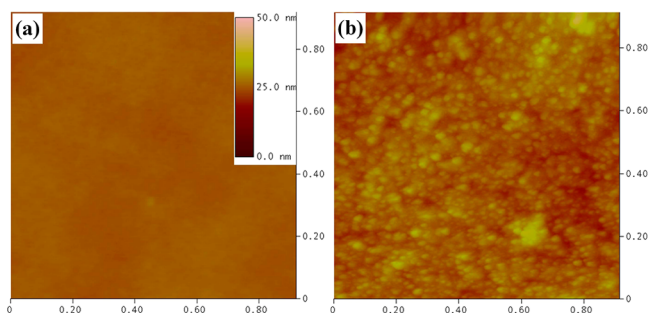


Figure 1. AFM images of the PDMAEMA brushes (a) before and (b) after the incorporation of Au NPs. Size are $0.9 \mu\text{m} \times 0.9 \mu\text{m}$.

root-mean-square (rms) roughness was measured as 0.45 nm for the bare polymer brush surface, and increased apparently to 2.49 nm for the hybrid films because of incorporation of Au NPs. The immobilized NPs are present in the form of domains, which is probably attributed to surface aggregation visually in the dry state and thus leads to the loss of uniformity.³⁹ Moreover, upon drying, the polymer brushes in the hybrid films present collapse state and bring adsorbed NPs close to each other.⁴⁰

The XPS characterization confirms the successful incorporation of Au NPs into PDMAEMA brushes (Figure 2). The

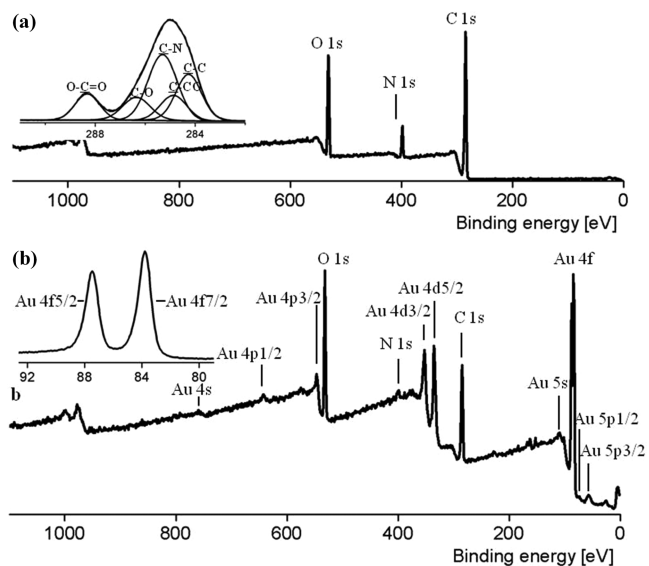


Figure 2. XPS wide-scan spectrum of (a) PDMAEMA brushes. Inset shows its C 1s core level spectrum. (b) PDMAEMA brushes immobilized Au NPs. Inset shows its Au 4f core level spectra.

presence of characteristic peak of Au 4f (Figure 2b) indicates the existence of Au compared with bare PDMAEMA brushes (Figure 2a). The binding energy for Au 4f7/2 and 4f5/2 have been measured as 87.4 and 83.8 eV respectively, which are consistent with Au⁰ oxidation state.³⁸

The Au NPs hardly aggregate and show good stability in the polymer brushes, as shown in TEM measurements. TEM

sample was prepared by dissolving the polymer brush/gold nanoparticles hybrid layer from the substrate by HF solution, and transferring the dispersed materials onto a carbon-coated Cu grid. Au NPs immobilized within the brushes is clearly visible and were well dispersed with an average diameter of 4.60 nm (Figure 3b). Compared with the initially synthetic Au NPs

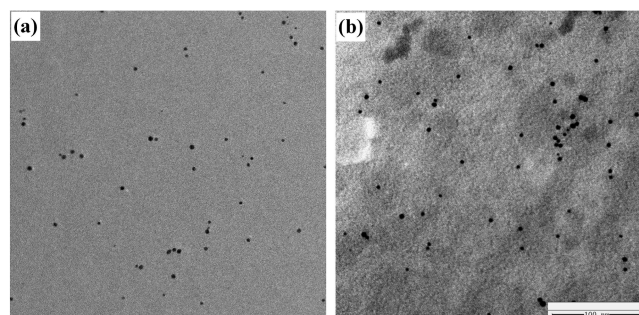


Figure 3. TEM images of (a) the synthetic Au NPs and (b) the dissolved Au NPs from the silica by HF solution.

with an average diameter of 4.52 nm (Figure 3a), the size and monodispersity of the dissolved Au NPs has negligible change, indicating the good stability of Au NPs in the polymer brushes.

Besides silicon substrate, the hybrid films can be grafted on flexional PET substrates and microcap with the aid of PDMAEMA brushes (Supporting Information Figure S2), which extends its applications.

Host–Guest Interaction between Au NPs and PDMAEMA Brushes. The inclusion complexation can be formed between side group of PDMAEMA and β -CD by host–guest interaction.²⁸ Thus, polymer brush/gold nanoparticles hybrid films can be fabricated based on host–guest interaction between β -CD cavity of gold nanoparticles and dimethylamino group of PDMAEMA (as shown in Figure 4a). The formation

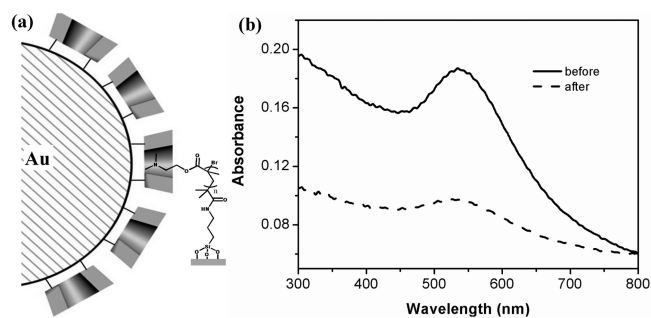


Figure 4. (a) Sketch of host–guest interaction between gold nanoparticles and PDMAEMA brush. (b) UV–vis absorption spectrum of PDMAEMA brushes immobilized Au NPs before and after immersing in DMAEMA monomer aqueous solution for 72 h.

of host–guest interaction between Au NPs and PDMAEMA brushes is confirmed by immersing the sample in DMAEMA monomer aqueous solution. The excessive DMAEMA monomer acts as competitive guest and water facilitates dissolution of Au NPs. The obvious decrease of absorption at 538 nm for the sample after addition of DMAEMA monomer aqueous solution demonstrates that most of Au NPs are displaced from polymer brushes and released back to solution (Figure 4b), which is attributed to dissociation of interaction between β -CD ligand of Au NPs and PDMAEMA brushes. Because of the existence of

many dimethylamino groups on PDMAEMA brushes, few Au NPs still remain on the polymer brushes (Figure 4b).

To investigate the influence factor on composite process, Au NPs have been incorporated by different composite time and different thickness of polymer brushes. Figure 5a shows that the

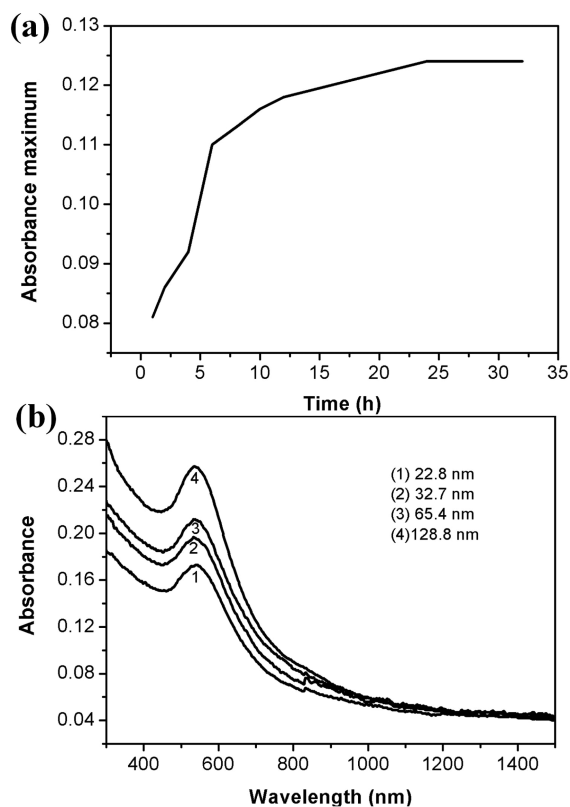


Figure 5. UV-vis absorption spectrum of PDMAEMA brush/Au NPs hybrid films with (a) different composite time and (b) different thickness of polymer brushes.

intensity of the absorbance band increases with the increase of composite time. The absorbance intensity increases fast at the beginning and then slows down after 5 h, and finally stops after 24 h. The phenomenon can be explained as follows: the Au NPs may mainly absorb on the surface rapidly at first, which is resulted from direct contact between Au NPs and polymer brushes. When the NPs occupy majority of the surface of the polymer brushes, the Au NPs have to permeate into polymer brushes by migrating themselves through breaking equilibrium of host-guest interaction, thus slowing down the speed of incorporation. After 24 h, the Au NPs may be hindered by the high density of polymer brushes and reach capacity. When incorporation time were immobilized at 8 h, by increasing thickness of polymer brushes from 22.8 to 128.8 nm, the intensity of absorbance bands increase in the meantime, which is attributed to increment of absorbed Au NPs (Figure 5b). The absorption bands of the different thickness of hybrid films remain about the same, indicating almost no aggregation of the Au NPs in the polymer films. It is further confirmed by characterization of thickness difference between PDMAEMA brushes and corresponding PDMAEMA/Au hybrid films, and the thickness difference increases with the increase of the thickness of polymer brushes (Supporting Information Table S1). This is because thick polymer brushes can provide more binding sites and have good swinging flexibility. The thickness

increments are 26.9, 34.2, 37.3, and 42.8 nm, respectively, after introduction of gold nanoparticles, which are larger than the diameter of gold nanoparticles, indicating a multilayer infiltration of gold nanoparticles in polymer brushes.

Tunable Structure and Optical Property for the Gold Nanoparticle Arrays. The fabrication process for polymer brush/gold nanoparticles hybrid nanoarrays is outlined in Figure 6. First, the PDMAEMA brushes were grown on silicon

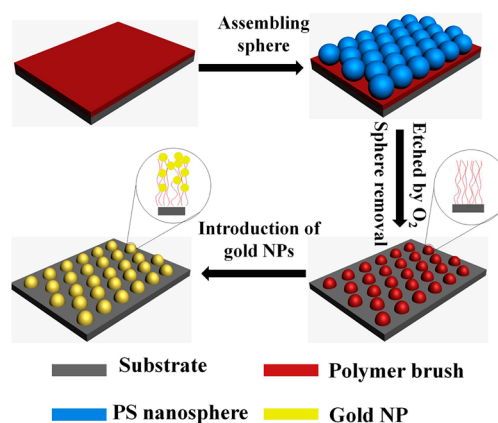


Figure 6. Procedure of fabricating polymer brush/Au NP hybrid nanoarrays by host-guest interaction.

substrates by ATRP reaction. Then, a 2D PS colloidal crystal was prepared by the modified interface method on the substrate with a film of PDMAEMA brush, and subsequently the PDMAEMA brush patterns were fabricated by oxygen RIE using 2D PS colloidal crystal as masks. At last, the patterned polymer brush/gold nanoparticles hybrid nanoarrays are obtained by immersing the above-mentioned sample in the solution of β -CD decorated gold nanoparticles for 8 h.

The nanostructures of PDMAEMA brushes/Au NP hybrid arrays can be precisely controlled by varying etching time. Figure 7 shows AFM images of PDMAEMA/Au NP hybrid arrays by etching PDMAEMA brush films with a thickness of 160 nm for 240 s (Figure 7a), 300 s (Figure 7b), 360 s (Figure 7c) and 420s (Figure 7d) using a 2D PS colloidal crystal of 580 nm in period as masks. In the process of colloidal lithography, the PS colloidal crystal is etched by oxygen plasma first and then the PDMAEMA brush films without the protection of PS spheres are etched by oxygen plasma. With the increasing of the etching time, the PS spheres become small and the voids become large, which results in small polymer brush nanodots after removing the mask of PS microspheres. The change of morphology of PDMAEMA/Au hybrid nanopatterns (Figure 7a-d) comply with similar trend with polymer brush nanodots. When polymer brushes were etched for 240 s and integrated with Au NPs, the bridged hybrid film patterns are formed on the substrate with height about 222 nm. When etching time increases to 300, 360, and 420 s, the height decreases to 189, 159, and 124 nm, and the diameter correspondingly decreases to 472, 426, and 433 nm, respectively, in the meantime. Cross-sectional profiles shows that all hybrid film patterns exhibit tapered profile the same as polymer brush patterns,⁴¹ so various gold nanoparticle arrays can be fabricated by patterned polymer brushes with various morphology and structure.

The influences of different structures on absorption spectra of the prepared gold nanoparticle arrays are shown in Figure 7e and f. All the structures present an absorption peak around 538

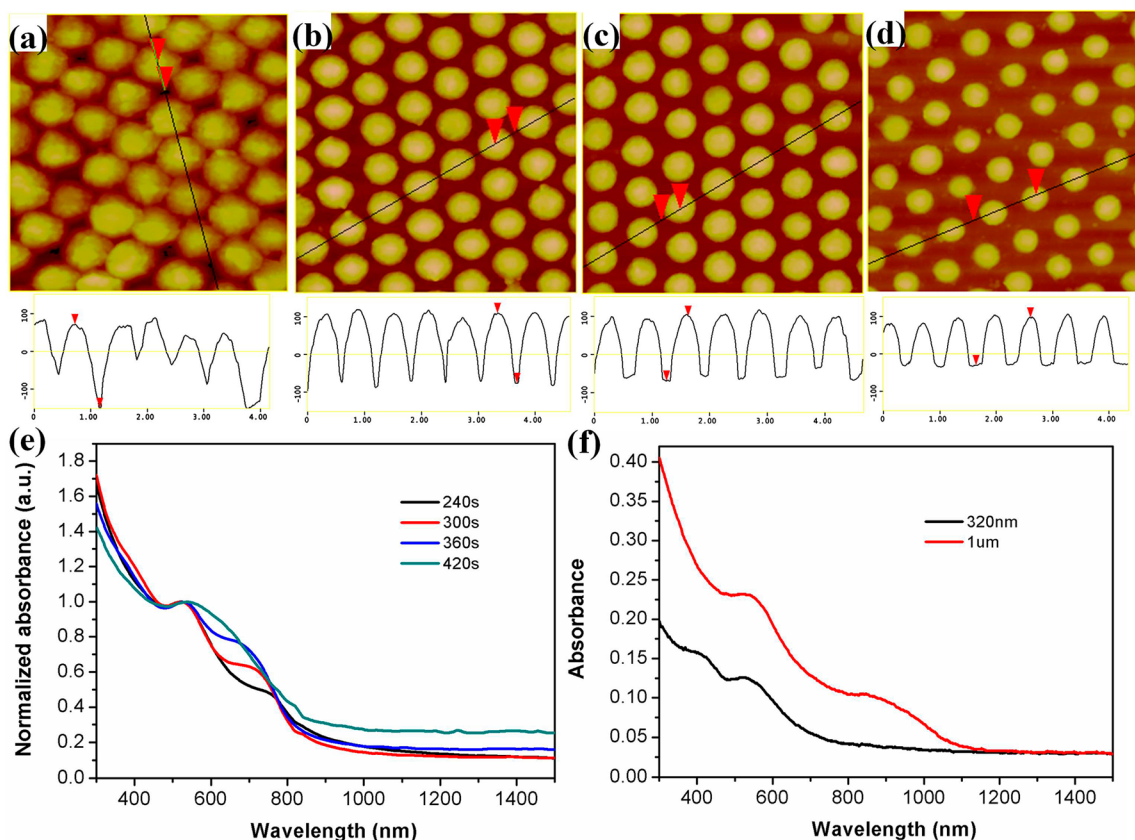


Figure 7. AFM images and cross-sectional profiles of PDMAEMA nanopatterns/Au hybrid films by etching PDMAEMA brush films with a thickness of 160 nm for (a) 240, (b) 300, (c) 360, and (d) 420s, sizes are $4\ \mu\text{m} \times 4\ \mu\text{m}$. UV-vis spectra of PDMAEMA nanopatterns/Au hybrid films by etching PDMAEMA brush films of 160 nm (e) for different time using 580 nm colloid sphere as mask and (f) using 320 nm and $1\ \mu\text{m}$ colloid sphere as mask to etch certain time.

nm, which is assigned to Au NPs resonance coupled via nonpropagating localized surface plasmons.⁵ In addition to this coupled nanoparticles cluster resonance, another absorption peak (λ_s) in the appears, and the appearance of λ_s is ascribed to interaction between the surface plasmon resonance effects of the Au NPs and bragg scattering of the ordered nanoarrays.^{4,7,42} The location of the λ_s can be controlled by varying the structure parameters of the patterns. For the nanopatterns with a period of 580 nm, the λ_s is blue-shifted from 761 to 716 nm, 691 nm, and until partly overlapping with 538 nm absorption peak and showing as a broaden absorption peak respectively with the decrease of feature size (as shown in Figure 7e). For the nanopatterns with a period of 320 nm and $1\ \mu\text{m}$, λ_s can be adjusted to shorter wavelength region and near-infrared region, respectively (Figure 7f). More tunable optical properties can be presented by changing periods, heights, and distances between two gold nanocluster dots of the hybrid nanoarrays.

4. CONCLUSION

We provides a versatile, low-cost, and very efficient method to fabricate nanoscale patterns of nanoparticles. Polymer brush/gold NPs hybrid nanoarrays are fabricated based on host-guest interaction between β -CD cavity on the gold nanoparticles and dimethylamino group of PDMAEMA. The gold nanoparticles present good stability in the polymer brushes. The influence factor of composite process has been discussed, including composite time and thickness of polymer brushes. By the use of colloidal lithography, the structures of gold nanoparticle arrays mediated by polymer brushes can be tuned. Besides, the spectra

of gold nanoparticle arrays varies from visible region to near-infrared region various with the control of structure parameters. The polymer brush/Au NP hybrid nanoarrays can be fabricated by combining different polymer brush patterns, such as elliptical nanorings and nanodiscs, stripes, and hierarchical patterns,^{41,43,44} and this complicated hybrid structures will bring about new optical properties. Moreover, arbitrary nanoparticles modified by β -CD such as semiconductor nanocrystals and magnetic nanoparticles can be introduced into the patterned polymer brushes, and various patterned hybrid materials with different functions can be fabricated. We believe that these materials are very useful in sensors, surface enhanced spectroscopy, magnetic storage device, antifake application, and biointerfaces.

■ ASSOCIATED CONTENT

Supporting Information

UV-vis absorption spectrum of Au NPs and PDMAEMA brush/Au hybrid films, thickness of the PDMAEMA brushes, corresponding hybrid films after incorporation of Au NPs, and the thickness difference between them; Photographs of PDMAEMA brush/Au NPs hybrid films on PET substrate and microcap. This material is available free of charge via the Internet at <http://pubs.acs.org>.

■ AUTHOR INFORMATION

Corresponding Author

*E-mail: byangchem@jlu.edu.cn. Fax: +86 431 85193423.

Author Contributions

The manuscript was written through contributions of all authors. All authors have given approval to the final version of the manuscript.

Notes

The authors declare no competing financial interest.

ACKNOWLEDGMENTS

This work was financially supported by the National Science Foundation of China (NSFC) under Grant No. 91123031, 21221063, 51373065, and the National Basic Research Program of China (973 Program) under Grant No. 2012CB933800.

REFERENCES

- (1) Anker, J. N.; Hall, W. P.; Lyandres, O.; Shah, N. C.; Zhao, J.; Van Duyne, R. P. Biosensing with Plasmonic Nanosensors. *Nat. Mater.* **2008**, *7*, 442–453.
- (2) Konstantatos, G.; Sargent, E. H. Nanostructured Materials for Photon Detection. *Nat. Nano* **2010**, *5*, 391–400.
- (3) Yang, B.; et al. Tuning the Intensity of Metal-Enhanced Fluorescence by Engineering Silver Nanoparticle Arrays. *Small* **2010**, *6*, 1038–1043.
- (4) Yan, B.; Thubagere, A.; Premasiri, W. R.; Ziegler, L. D.; Dal Negro, L.; Reinhard, B. M. Engineered SERS Substrates with Multiscale Signal Enhancement: Nanoparticle Cluster Arrays. *ACS Nano* **2009**, *3*, 1190–1202.
- (5) Stewart, M. E.; Anderton, C. R.; Thompson, L. B.; Maria, J.; Gray, S. K.; Rogers, J. A.; Nuzzo, R. G. Nanostructured Plasmonic Sensors. *Chem. Rev.* **2008**, *108*, 494–521.
- (6) Vazquez-Mena, O.; Sannomiya, T.; Villanueva, L. G.; Voros, J.; Brugger, J. Metallic Nanodot Arrays by Stencil Lithography for Plasmonic Biosensing Applications. *ACS Nano* **2010**, *5*, 844–853.
- (7) Li, J.-H.; Chen, S.-W.; Chou, Y.; Wu, M.-C.; Hsueh, C.-H.; Su, W.-F. Effects of Gold Film Morphology on Surface Plasmon Resonance Using Periodic P3ht:Pmma/Au Nanostructures on Silicon Substrate for Surface-Enhanced Raman Scattering. *J. Phys. Chem. C* **2011**, *115*, 24045–24053.
- (8) Jain, P. K.; Huang, W.; El-Sayed, M. A. On the Universal Scaling Behavior of the Distance Decay of Plasmon Coupling in Metal Nanoparticle Pairs: A Plasmon Ruler Equation. *Nano Lett.* **2007**, *7*, 2080–2088.
- (9) Shankar, S. S.; Rizzello, L.; Cingolani, R.; Rinaldi, R.; Pompa, P. P. Micro/Nanoscale Patterning of Nanostructured Metal Substrates for Plasmonic Applications. *ACS Nano* **2009**, *3*, 893–900.
- (10) Haynes, C. L.; Van Duyne, R. P. Nanosphere Lithography: A Versatile Nanofabrication Tool for Studies of Size-Dependent Nanoparticle Optics. *J. Phys. Chem. B* **2001**, *105*, 5599–5611.
- (11) Gao, B.; Rozin, M. J.; Tao, A. R. Plasmonic Nanocomposites: Polymer-Guided Strategies for Assembling Metal Nanoparticles. *Nanoscale* **2013**, *5*, 5677.
- (12) Aizawa, M.; Buriak, J. M. Block Copolymer-Templated Chemistry on Si, Ge, Inp, and Gaas Surfaces. *J. Am. Chem. Soc.* **2005**, *127*, 8932–8933.
- (13) Orilall, M. C.; Wiesner, U. Block Copolymer Based Composition and Morphology Control in Nanostructured Hybrid Materials for Energy Conversion and Storage: Solar Cells, Batteries, and Fuel Cells. *Chem. Soc. Rev.* **2011**, *40*, 520–535.
- (14) Barbey, R.; Lavanant, L.; Paripovic, D.; Schüwer, N.; Sugnaux, C.; Tugulu, S.; Klok, H.-A. Polymer Brushes Via Surface-Initiated Controlled Radical Polymerization: Synthesis, Characterization, Properties, and Applications. *Chem. Rev.* **2009**, *109*, 5437–5527.
- (15) Ramesh, G. V.; Porel, S.; Radhakrishnan, T. P. Polymer Thin Films Embedded with in Situ Grown Metal Nanoparticles. *Chem. Soc. Rev.* **2009**, *38*, 2646–2656.
- (16) Ducker, R.; Garcia, A.; Zhang, J.; Chen, T.; Zauscher, S. Polymeric and Biomacromolecular Brush Nanostructures: Progress in

Synthesis, Patterning and Characterization. *Soft Matter* **2008**, *4*, 1774–1786.

- (17) Gupta, S.; Agrawal, M.; Uhlmann, P.; Simon, F.; Stamm, M. Poly(*N*-Isopropyl Acrylamide)–Gold Nanoassemblies on Macroscopic Surfaces: Fabrication, Characterization, and Application. *Chem. Mater.* **2009**, *22*, 504–509.

- (18) Oren, R.; Liang, Z.; Barnard, J. S.; Warren, S. C.; Wiesner, U.; Huck, W. T. S. Organization of Nanoparticles in Polymer Brushes. *J. Am. Chem. Soc.* **2009**, *131*, 1670–1671.

- (19) Mejia-Ariza, R.; Huskens, J. Formation of Hybrid Gold Nanoparticle Network Aggregates by Specific Host-Guest Interactions in a Turbulent Flow Reactor. *J. Mater. Chem. B* **2014**, *2*, 210–216.

- (20) Gehan, H.; Fillaud, L.; Chehimi, M. M.; Aubard, J.; Hohenau, A.; Felidj, N.; Mangeney, C. Thermo-Induced Electromagnetic Coupling in Gold/Polymer Hybrid Plasmonic Structures Probed by Surface-Enhanced Raman Scattering. *ACS Nano* **2010**, *4*, 6491–6500.

- (21) Lee, S.; Pérez-Luna, V. H. Dextran–Gold Nanoparticle Hybrid Material for Biomolecule Immobilization and Detection. *Anal. Chem.* **2005**, *77*, 7204–7211.

- (22) Gupta, S.; Agrawal, M.; Conrad, M.; Hutter, N. A.; Olk, P.; Simon, F.; Eng, L. M.; Stamm, M.; Jordan, R. Poly(2-(Dimethylamino)Ethyl Methacrylate) Brushes with Incorporated Nanoparticles as a SERS Active Sensing Layer. *Adv. Funct. Mater.* **2010**, *20*, 1756–1761.

- (23) Klajn, R.; Olson, M. A.; Wesson, P. J.; Fang, L.; Coskun, A.; Trabolsi, A.; Soh, S.; Stoddart, J. F.; Grzybowski, B. A. Dynamic Hook-and-Eye Nanoparticle Sponges. *Nat. Chem.* **2009**, *1*, 733–738.

- (24) Yao, Y.; Zhou, Y.; Dai, J.; Yue, S.; Xue, M. Host-Guest Recognition-Induced Color Change of Water-Soluble Pillar[5]Arene Modified Silver Nanoparticles for Visual Detection of Spermene Analogues. *Chem. Commun.* **2014**, *50*, 869–871.

- (25) Ha, W.; Kang, Y.; Peng, S.-L.; Ding, L.-S.; Zhang, S.; Li, B.-J. Vesicular Gold Assemblies Based on Host–Guest Inclusion and Its Controllable Release of Doxorubicin. *Nanotechnology* **2013**, *24*, 495103–495110.

- (26) Leng, J.; Wen, X.; Rao, J.; Zou, G.; Zhang, Q. Thermal and pH Dual Stimuli-Responsive Hybrid Inclusion Complex with Tunable Nonlinear Optical Properties. *Polymer* **2012**, *53*, 1543–1550.

- (27) Hashidzume, A.; Harada, A. Recognition of Polymer Side Chains by Cyclodextrins. *Polym. Chem.* **2011**, *2*, 2146–2154.

- (28) Zhao, Y.; Guo, K.; Wang, C.; Wang, L. Effect of Inclusion Complexation with Cyclodextrin on the Cloud Point of Poly(2-(Dimethylamino)Ethyl Methacrylate) Solution. *Langmuir* **2010**, *26*, 8966–8970.

- (29) Ritter, H.; Sadowski, O.; Tepper, E. Influence of Cyclodextrin Molecules on the Synthesis and the Thermoresponsive Solution Behavior of *N*-Isopropylacrylamide Copolymers with Adamantyl Groups in the Side-Chains. *Angew. Chem., Int. Ed.* **2003**, *42*, 3171–3173.

- (30) Pyun, J.; Kowalewski, T.; Matyjaszewski, K. Synthesis of Polymer Brushes Using Atom Transfer Radical Polymerization. *Macromol. Rapid Commun.* **2003**, *24*, 1043–1059.

- (31) Yang, S. H.; Park, J. H.; Cho, W. K.; Lee, H.-S.; Choi, I. S. Counteranion-Directed, Biomimetic Control of Silica Nanostructures on Surfaces Inspired by Biosilicification Found in Diatoms. *Small* **2009**, *5*, 1947–1951.

- (32) Yang, S. H.; Kang, K.; Choi, I. S. Biomimetic Approach to the Formation of Titanium Dioxide Thin Films by Using Poly(2-(Dimethylamino)Ethyl Methacrylate). *Chem.—Asian J.* **2008**, *3*, 2097–2104.

- (33) Löbbecke, R.; Chanana, M.; Schlaad, H.; Pilz-Allen, C.; Günter, C.; Möhwald, H.; Taubert, A. Polymer Brush Controlled Bioinspired Calcium Phosphate Mineralization and Bone Cell Growth. *Bio-macromolecules* **2011**, *12*, 3753–3760.

- (34) Dinh, C.-T.; Yen, H.; Kleitz, F.; Do, T.-O. Three-Dimensional Ordered Assembly of Thin-Shell Au/TiO₂ Hollow Nanospheres for Enhanced Visible-Light-Driven Photocatalysis. *Angew. Chem., Int. Ed.* **2014**, *53*, 6618–6623.

- (35) Zhang, Z.; Zhang, L.; Hedhili, M. N.; Zhang, H.; Wang, P. Plasmonic Gold Nanocrystals Coupled with Photonic Crystal Seamlessly on TiO₂ Nanotube Photoelectrodes for Efficient Visible Light Photoelectrochemical Water Splitting. *Nano Lett.* **2012**, *13*, 14–20.
- (36) Li, Y.; Zhang, J.; Zhu, S.; Dong, H.; Wang, Z.; Sun, Z.; Guo, J.; Yang, B. Bioinspired Silicon Hollow-Tip Arrays for High Performance Broadband Anti-Reflective and Water-Repellent Coatings. *J. Mater. Chem.* **2009**, *19*, 1806–1810.
- (37) Liu, J.; Ong, W.; Román, E.; Lynn, M. J.; Kaifer, A. E. Cyclodextrin-Modified Gold Nanospheres. *Langmuir* **2000**, *16*, 3000–3002.
- (38) Brust, M.; Walker, M.; Bethell, D.; Schiffrin, D. J.; Whyman, R. Synthesis of Thiol-Derivatized Gold Nanoparticles in a Two-Phase Liquid-Liquid System. *J. Chem. Soc., Chem. Commun.* **1994**, 801–802.
- (39) Malynych, S.; Luzinov, I.; Chumanov, G. Poly(Vinyl Pyridine) as a Universal Surface Modifier for Immobilization of Nanoparticles. *J. Phys. Chem. B* **2002**, *106*, 1280–1285.
- (40) Gupta, S.; Uhlmann, P.; Agrawal, M.; Chapuis, S.; Oertel, U.; Stamm, M. Immobilization of Silver Nanoparticles on Responsive Polymer Brushes. *Macromolecules* **2008**, *41*, 2874–2879.
- (41) Li, Y.; Zhang, J.; Liu, W.; Li, D.; Fang, L.; Sun, H.; Yang, B. Hierarchical Polymer Brush Nanoarrays: A Versatile Way to Prepare Multiscale Patterns of Proteins. *ACS Appl. Mater.* **2013**, *5*, 2126–2132.
- (42) Félidj, N.; Aubard, J.; Lévi, G.; Krenn, J. R.; Schider, G.; Leitner, A.; Aussenegg, F. R. Enhanced Substrate-Induced Coupling in Two-Dimensional Gold Nanoparticle Arrays. *Phys. Rev. B* **2002**, *66*, 245407.
- (43) Liu, W.; Li, Y.; Wang, T.; Li, D.; Fang, L.; Zhu, S.; Shen, H.; Zhang, J.; Sun, H.; Yang, B. Elliptical Polymer Brush Ring Array Mediated Protein Patterning and Cell Adhesion on Patterned Protein Surfaces. *ACS Appl. Mater.* **2013**, *5*, 12587–12593.
- (44) Chen, T.; Amin, I.; Jordan, R. Patterned Polymer Brushes. *Chem. Soc. Rev.* **2012**, *41*, 3280–3296.